

# Experimental Investigation of the Friction and Wear Behaviour with an Adapted Ball-On-Prism Test Setup

V. Krasmik<sup>a</sup>, J. Schlattmann<sup>a</sup>

<sup>a</sup> *Workgroup on System Technologies and Engineering Design Methodology, Hamburg University of Technology, 21073 Hamburg, Germany.*

## Keywords:

*Coefficient of friction  
Wear rate  
Tribological testing  
Ball-on-prism test setup  
Number of contact points  
Copper  
Brass*

## ABSTRACT

*In this study, the friction and wear behaviour of a brass-steel and a copper-steel pairing is investigated and compared. For this purpose, an adapted ball-on-prism test configuration is used. With the proposed test setup, the evolution of the coefficient of friction and the surface temperature, as well as, the linear wear rate and the weight loss are obtained. The influence of the normal load, the sliding velocity, and the number of contact points are examined. The results for the brass-steel pairing reveal no dependency of the coefficient of friction on the normal load and the number of contact points, whereas for higher sliding velocities, a slight increase of the coefficient of friction can be observed. The linear wear rate increases with the normal load, the sliding velocity, and the number of contact points. The coefficient of friction for the copper-steel pairing decreases with an increase of the normal load, increases for higher sliding velocities, and shows no obvious dependency on the number of contact points. The linear wear rate decreases with increasing sliding velocity and increases with the number of contact points.*

## Corresponding author:

*Viktor Krasmik  
Workgroup on System Technologies  
and Engineering Design  
Methodology, Hamburg University of  
Technology, 21073 Hamburg,  
Germany.  
E-mail: viktor.krasmik@tuhh.de*

© 2015 Published by Faculty of Engineering

## 1. INTRODUCTION

Whenever solid bodies are in relative motion to each other, frictional resistance at the contact surface opposes the motion, and wear processes are very likely to occur. The performance (efficiency and durability) of mechanical systems (like brakes, clutches, joints, etc.) with regard to friction and wear is highly influenced by the surface interaction in the contact regions of the nominal contact area.

For the characterization of the friction and wear behaviour, different testing approaches exist. They are considered to be dependent on the scale and complexity of the system under investigation [1-3]. Whereas field tests are necessary for the final proof of the transferability of the gained conclusions to real systems, model or laboratory tests are used to reproduce a particular tribological situation and to understand the fundamental influence of relevant parameters, like the normal load or the sliding velocity.

For the highest level of abstraction, test setups like pin-on-disk, block-on-ring, ball-on-plate, ball-on-three-balls, ball-on-prism, and many more have been developed and are widely used for studying and characterizing the friction and wear behaviour [3].

The results of several studies [4-7] show that friction and wear depend on normal load, sliding velocity, contact geometry, surface roughness, material pairing, dynamics of the system, lubrication, temperature, and relative humidity.

De Moerlooze et al. [8] used a rotational ball-on-flat setup to study the effect of normal load. For steel-steel and steel-alumina pairings, a linear trend for the wear volume and the dissipated energy as a function of the normal load was observed.

Chowdhury et al. [9] and Chowdhury and Nuruzzaman [10,11] used a pin-on-disk setup to investigate the normal load and sliding velocity dependency. For copper-brass and steel-steel pairings, it was observed that the coefficient of friction decreases for higher normal loads and increases for higher sliding velocities. For aluminium-steel pairings, on the other hand, the coefficient of friction decreases with increasing normal load and sliding velocity. Furthermore, higher wear rates were observed with increased normal loads and sliding velocities.

Using a ball-on-three-disk test method, Fildes et al. [12] studied the wear and abrasion resistance of different hard coatings. The results demonstrated the performance benefits of many modern coatings and the effect of different coating design strategies on abrasive and adhesive wear.

Generally, it can be said that the friction and wear characteristics of metals and alloys strongly depend on the testing conditions. In this context, many investigations using different test methods and parameters for different material pairings have been conducted [3]. Nevertheless, not for all model test systems, the friction and wear behaviour regarding the normal load and the sliding velocity dependency is known.

According to ISO 7148-2 [13], the ball-on-prism setup is primarily designed for testing polymer-based plain bearing materials. The configuration

reproduces the conditions in a bearing bushing regarding the contact pressure and contact area. Due to the spherical contact geometry, it can be assumed that the contact pressure decreases, while the contact area increases with run time.

In this study, an adapted ball-on-prism contact configuration is used for studying the effect of normal load, sliding velocity, and number of contact points on the friction and wear behaviour of a brass-steel and a copper-steel pairing. Such material pairings and their related alloys are often used in many industrial applications. Some of the main reasons for this are their thermal and electrical properties, their wear and friction performance, and their corrosion resistance [14].

## 2. EXPERIMENTAL PROCEDURE

### 2.1 Materials and preparation

For the present study, samples with the dimensions of  $8 \times 5 \times 1$  mm were prepared from commercially available brass (CuZn37) and copper (SF-Cu) sheets. Steel balls (100Cr6) with a diameter of  $D = 12.7$  mm were used as the rotating counterpart. In Table 1, relevant properties of the used materials and the corresponding material numbers are listed.

**Table 1.** Properties of the used test samples.

Material	Hardness, HRC	$R_a$ [ $\mu\text{m}$ ]
CuZn37 (2.0321)	–	< 0.4
SF-Cu (2.0090)	–	< 0.4
100Cr6 (1.3505)	60 – 66	< 0.03

The samples were cleaned with a technical cleaner in an ultrasonic bath before the tests.

### 2.2 Contact configuration

In the proposed test setup, a ball is loaded against flat test samples positioned in a pyramid-like holder with an opening angle of  $90^\circ$ . The test samples are arranged on the circumference in a regular manner. The ball rotates uniformly around its vertical axis and slides over the samples. In Figure 1, the pyramid-like sample holders are shown. Contact configurations with two, three, and four samples, respectively contact points, were investigated.

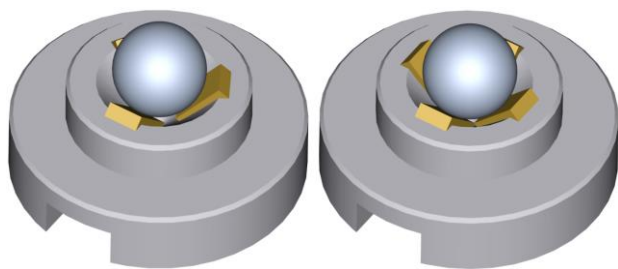


**Fig. 1.** Adapted ball-on-prism sample holder.

A slot and key principle was used to install the sample holder in the test bench, so that a self-adjustment of the pyramid with the samples with respect to the rotating ball was possible.

Additionally, the diameters of the wear spots of the samples were compared after the tests. If the size of these spots differed by more than 20 %, it was interpreted as an indication for an unequal load distribution, and the results were not considered for evaluation.

The steel ball was pressed with a defined load  $F_{Load}$  against the test samples. A schematic representation of the loading situation is given in Figure 2.

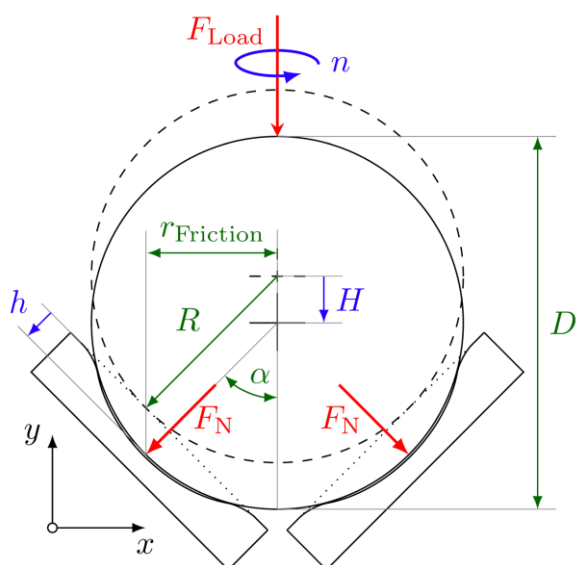


**Fig. 2.** Schematic representation of the loading configuration.

The resulting normal load acting on each test sample is:

$$F_N = \frac{F_{Load}}{n_{Contact} \cos \alpha}, \quad (1)$$

with  $n_{Contact}$  denoting the number of contact points, respectively test samples, and  $\alpha = 45^\circ$  the

half opening angle of the sample holder with respect to the loading direction of the applied load.

The sliding velocity is given by:

$$v = 2\pi n \frac{D}{2} \cos \alpha, \quad (2)$$

with  $n$  denoting the rotational speed.

The investigated loading configurations, the corresponding normal loads per sample, and the sliding velocities are given in Table 2.

**Table 2.** Investigated contact configurations and test parameters.

Number of contact points	Normal load per sample [N]	Sliding velocity [mm/s]
2	17.7, 35.4, 70.7	4.7, 9.4, 14.1
3	35.4	14.1
4	35.4	14.1

### 2.3 Experimental setup and procedure

A schematic representation of the used test bench is depicted in Figure 3. The holder for the rotating counterpart is connected to a servomotor. The pyramid-like holder with the test samples is installed on a vertically movable platform, which is connected to a motorized spindle by a lever mechanism. The normal load is applied by moving the lower platform in the upward direction. During the test, the applied load is measured continuously, and a force feedback controller is used to ensure a constant load.

The resulting friction force between the rotating ball and the flat samples is measured by a force sensor (deflection of an elastic arm equipped with strain gages), which is installed between a lever connected to the pyramid holder and the frame of the test bench.

The kinetic coefficient of friction was calculated by considering the friction radius  $r_{Friction}$ , the arm length  $r_{Sensor}$ , describing the distance between the rotational axis and the force sensor, the normal load  $F_N$ , and the measured force at the force sensor  $F_{Sensor}$ :

$$\mu = \frac{r_{Sensor} F_{Sensor}}{r_{Friction} F_N} = \frac{r_{Sensor} F_{Sensor}}{\frac{D}{2} \cos \alpha F_N}. \quad (3)$$

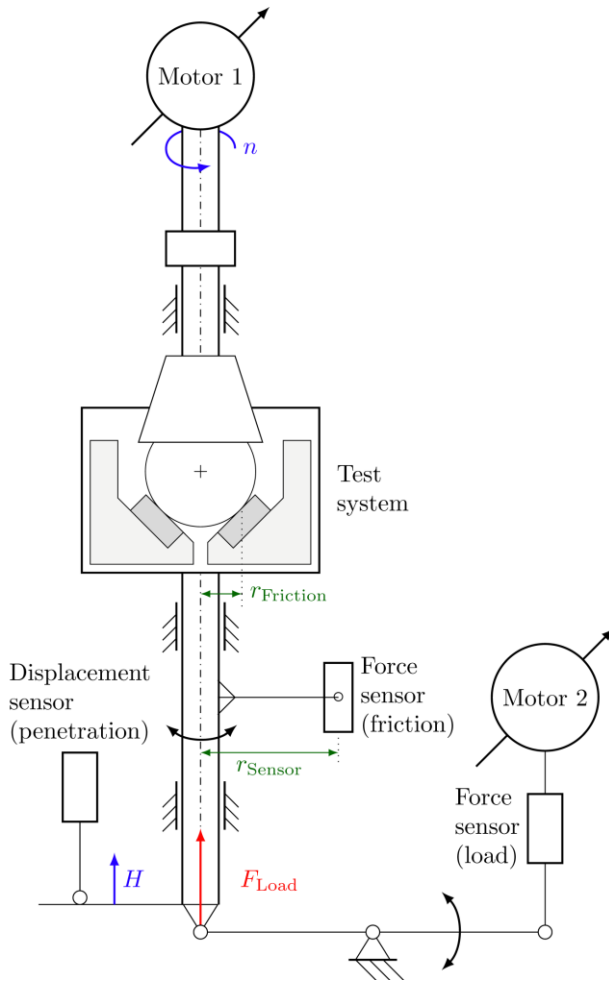


Fig. 3. Schematic representation of the test bench.

After passing an initial running-in phase, the coefficient of friction fluctuated around a roughly constant level. For evaluation, the average value for the last two-thirds of the total sliding distance was calculated.

A displacement sensor continuously measured the approach of the sample holder towards the holder of the rotating counterpart indicating the penetration of the rotating ball into the samples due to wear.

The results showed that both the flat samples and the balls wear out. Therefore, the penetration depth and not the volume loss are considered for evaluation.

The relation between the measured vertical displacement  $H$  and the penetration depth  $h$  is illustrated in Figure 2 and can be obtained with the following relation:

$$h = \cos\alpha H. \quad (4)$$

After an initial running-in period, all wear curves showed approximately a linear evolution. In Figure 4, two typical curves for the evolution of the penetration depth are presented. In order to evaluate the obtained curves, the linear part was approximated by the following linear function:

$$h_{\text{linear}}(s) = h_0 + w_{h,s}s, \quad (5)$$

with  $h_0$  representing the wear during the running-in phase and  $w_{h,s}$  the slope of the curve, respectively the linear wear rate, with respect to the sliding distance. In this context, the linear wear rate represents the combined wear behaviour of the flat samples and the steel ball. For the linear fitting, only the last two-thirds of the total sliding distance were taken into account.

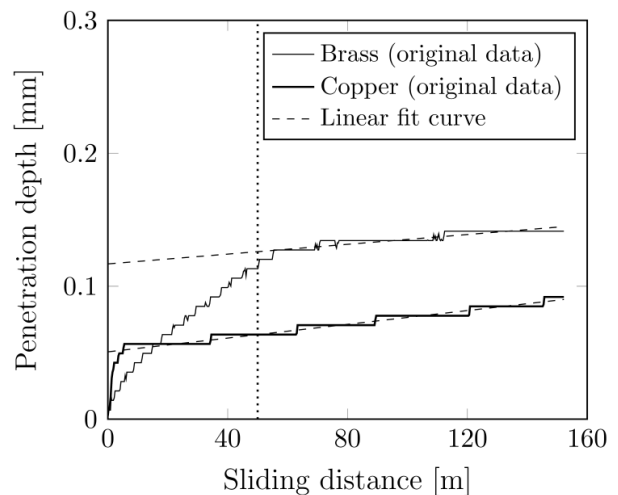


Fig. 4. Penetration depth curve for brass and copper.

In comparison to testing polymer-based materials where the wear of the rotating counterpart can usually be neglected, it is not the case for testing metal-metal pairings. Therefore, the weight loss of the steel balls was captured. For that purpose, an electronic balance was used for measuring the weight of the steel balls before and after the tests. A wear rate for the steel balls was not calculated since it cannot be assumed that the weight loss of the steel balls has a linear character, and therefore, only the total average weight loss was considered for evaluation. The weight loss of the flat samples was typically less than 1 mg and was hence not further considered.

Using flat thermocouples installed on the samples in the vicinity of the contact points, the evolution of the surface temperature of the samples was

monitored during the tests. After an initial rising, the temperatures reached a stationary level with no markedly changes. For this reason, the average temperature for the last two-thirds of the sliding distance was calculated for evaluation.

The duration of the tests was adapted according to the sliding velocities so that for all studied cases, the resulting total sliding distance was approximately  $s = 153$  m and the corresponding number of revolutions  $N = 5400$ .

A computer was used to define the test parameters (normal load, rotational speed, and test duration) and to record and process the measured signals (normal force, friction force, linear displacement, and temperature).

All tests were conducted under dry conditions at a room temperature of 21 °C and a relative humidity of 20 %. The tests were repeated at least three times for every parameter and contact configuration.

The raw data were averaged over 10 revolutions to compensate irregularities. The presented results in this contribution are the arithmetic mean values of the measured values, unless otherwise stated. The standard deviations of the mean values are indicated by error bars, illustrating the scatter of the results.

Before starting the friction and wear tests, some material pairings were loaded for 180 min with a static load and no rotating speed to investigate plastic deformation and creep effects. The resulting total creep deformation was only a few microns compared to the penetration due to wear during the friction and wear tests. Therefore, creep deformations were not considered in the following tests.

### 3. RESULTS AND DISCUSSION

#### 3.1 Effect of the normal load

In Figure 5, the effect of the normal load on the average coefficient of friction and the average temperature is illustrated.

The coefficient of friction for the brass-steel pairing shows no normal load dependency. This observation is in good agreement with Amonton-

Coulomb's law, which states that the friction force is proportional to the normal load for sliding solids under dry conditions. For the copper-steel pairing, a slight decrease of the coefficient of friction for higher normal loads can be observed. For identical conditions, it is evident that the coefficient of friction for the brass-steel pairing is smaller than for the copper-steel pairing.

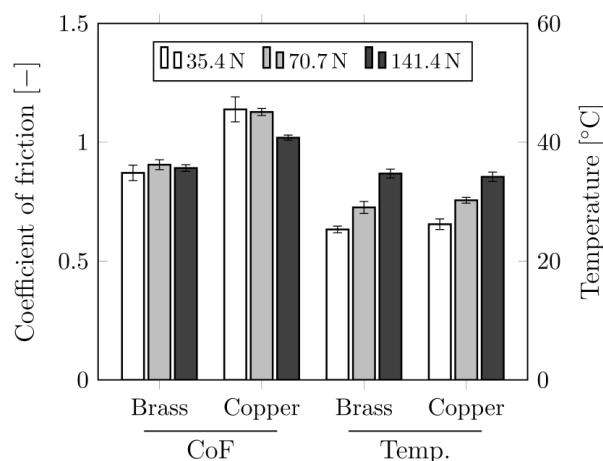


**Fig. 5.** Average coefficient of friction and temperature as a function of normal load for the brass-steel and copper-steel pairing ( $v = 14.1$  mm/s, two contact points).

Frictional interaction between sliding bodies leads to heat generation and a rise of the temperature at the contact surface. For both pairings, the average temperature increases with the normal load. The absolute values are almost on the same level.

The variation of the wear rate and the weight loss of the steel balls for different normal loads is shown in Figure 6. For the brass-steel pairing, an increase of the normal load leads to an increase of the wear rate and the weight loss of the steel balls. It is a common understanding that the real contact area is directly proportional to the normal load. Consequently, it means that for higher normal loads, a higher wear rate can be expected.

For the copper-steel pairing, however, the case is different. While the weight loss increases with the normal load, the linear wear rate shows no clear trend.

Due to the opening angle of the pyramid-like sample holder, loose wear debris could escape from the contact area and accumulate at the

bottom. Because of the ploughing effect and the surface roughening, some wear debris was still trapped in the worn spots. In Figure 7, the wear spots on a brass and a copper sample are illustrated.

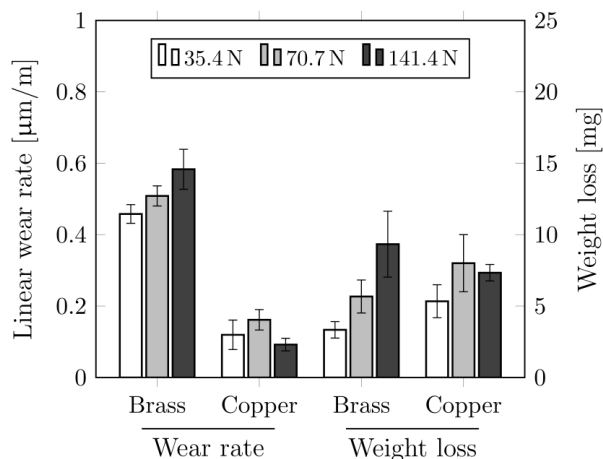


**Fig. 6.** Wear rate and weight loss as a function of normal load for the brass-steel and copper-steel pairing ( $v = 14.1 \text{ mm/s}$ , two contact points).

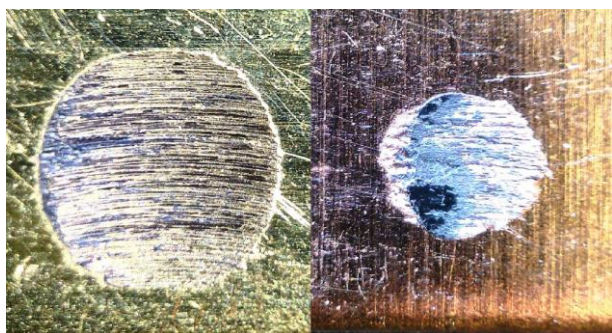


**Fig. 7.** Resulting wear spots on a brass (left) and a copper sample (right).

Especially for the copper-steel pairing, a formation of a layer at the rubbing regions on the flat samples was observed. This layer separates the contacting surfaces and affects the friction and wear behaviour. Temporary drops in the evolution of the coefficient of friction during the tests suggest that this layer breaks down and builds up again. For the brass-steel pairing, such a layer formation was only occasionally noticed.

The wear rate is almost three times higher for the brass-steel pairing than for the copper-steel pairing, whereas the weight losses are in a similar range. It is very likely that for the copper-steel pairing, the formed layer acted as a wear reduction mechanism and therefore explains the considerably smaller wear rates.

### 3.2 Effect of the sliding velocity

The average values of the coefficient of friction and the temperature as a function of the sliding velocity are illustrated in Figure 8.

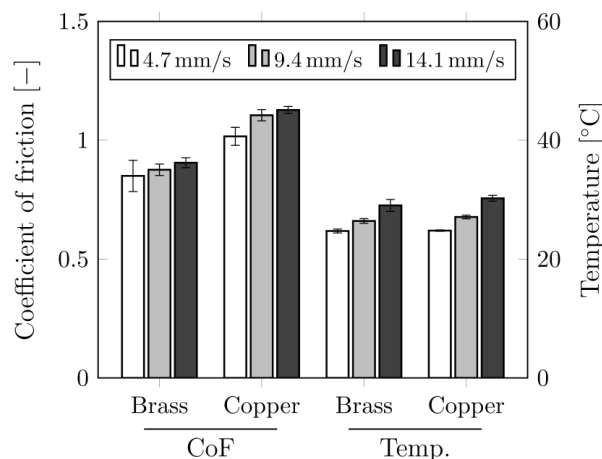


**Fig. 8.** Average coefficient of friction and temperature as a function of sliding velocity for the brass-steel and copper-steel pairing ( $F_N = 35.4 \text{ N}$ , two contact points).

For both pairings, the coefficient of friction and the average temperature increase with increasing sliding velocity. The coefficient of friction for the copper-steel pairing is higher than for the brass-steel pairing. An increase in the sliding velocity generates more heat, which is confirmed by the results.

For the study of different sliding velocities, the test duration was adapted so that the sliding distance was identical for all tests. The Figure 9 shows the effect of the sliding velocity on the wear behaviour.

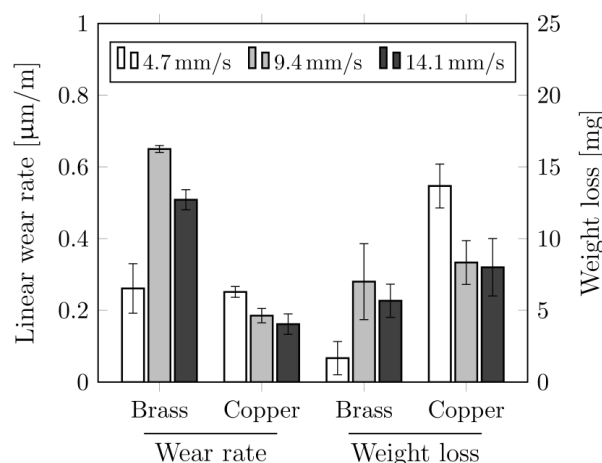


**Fig. 9.** Wear rate and weight loss as a function of sliding velocity for the brass-steel and copper-steel pairing ( $F_N = 35.4 \text{ N}$ , two contact points).

For the copper-steel pairing, the wear rate and the weight loss decrease for higher sliding velocities, whereas for the brass-steel pairing, the opposite is true, although for  $v = 9.4$  mm/s, a deviation can be observed. While the wear rate for the brass-steel pairing is higher compared to the copper-steel pairing, the weight loss is smaller. For higher sliding velocities, the formation of the layer is probably accelerated, which obviously increases friction and reduces wear.

### 3.3 Effect of the number of contact points

According to Amonton-Coulomb's law, the friction force is independent of the apparent contact area between two sliding solids under dry conditions. The results in Figure 10 show that no noticeable dependency between the coefficient of friction and the number of contact points exists, and therefore, the law is confirmed.

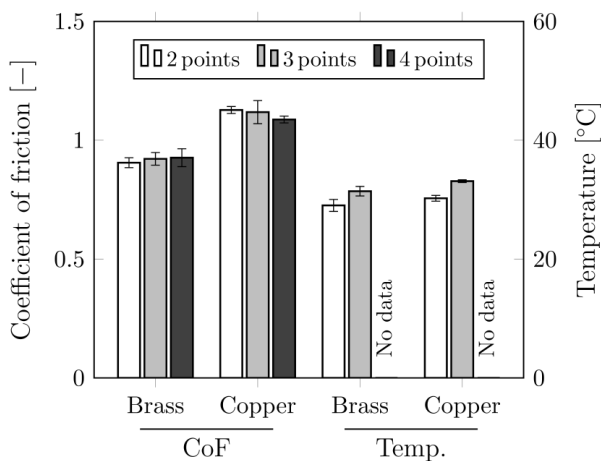


**Fig. 10.** Average coefficient of friction and temperature as a function of the number of contact points for the brass-steel and copper-steel pairing ( $F_N = 35.4$  N,  $v = 14.1$  mm/s).

The average temperature was only obtained for two and three contact points. Nevertheless, the results suggest an increase of the temperature with the number of contact points.

During all tests, the sliding distance experienced by each flat sample was always the same. For the configuration with two contact points, the sliding distance covered by the steel ball is twice as long as the distance covered by each sample. By doubling the number of contact points, the effective sliding distance covered by the steel ball also doubles. Therefore, increasing the

number of contact points increases the sliding distance experienced by the ball, which should result in an increased weight loss. The results in Figure 11 agree with this expectation, but obviously show no linear relationship. An increasing trend for the wear rate as a function of the number of contact points can also be observed. This observation can probably be attributed to the change of the surface properties (e.g., surface roughening) of the steel balls due to the increased weight loss because of the increased sliding distance.

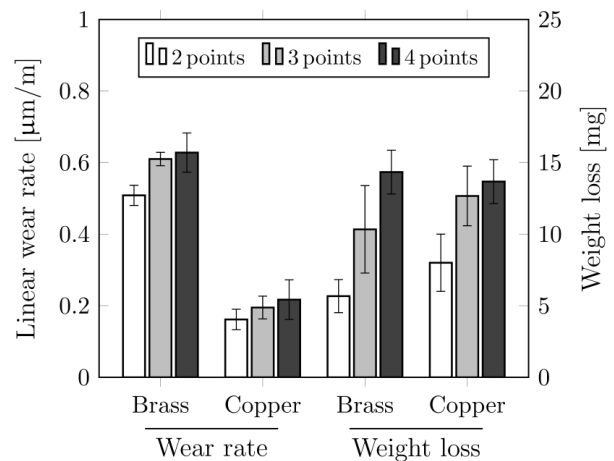


**Fig. 11.** Wear rate and weight loss as a function of the number of contact points for the brass-steel and copper-steel pairing ( $F_N = 35.4$  N,  $v = 14.1$  mm/s).

The weight loss of both material pairings is in the same range, whereas the absolute values of the wear rates differ by a factor of three.

### 4. CONCLUSION

In this study, an adapted ball-on-prism test setup was used to investigate the dependency of the wear and friction behaviour on the normal load, the sliding velocity, and the number of contact points for a brass-steel and a copper-steel pairing.

The coefficient of friction for the brass-steel pairing reveals no dependency on the normal load and the number of contact points and slightly increases for higher sliding velocities. The wear rate and the weight loss increase with increasing normal load, sliding velocity, and number of contact points.

For the copper-steel pairing, the coefficient of friction decreases for higher normal loads,

increases for higher sliding velocities, and shows no dependency on the number of contact points. The wear rate shows no clear dependency on the normal load, but decreases for higher sliding velocities and increases with the number of contact points. Furthermore, a formation of a protective layer on the flat copper samples has been observed. It is believed that this layer affects the overall performance and the dependency on the different loading parameters.

Compared to the brass-steel pairing, the coefficient of friction for the copper-steel pairing is higher and the wear rate is lower in the investigated parameter range and for identical conditions.

With the adapted ball-on-prism test setup, various material pairings under different loading conditions can be evaluated and compared. The setup allows a simple, cost-effective, and precise characterization of the friction and wear performance. The test setup can be easily extended for the investigation of lubricated contacts. For a more precise characterization of the wear performance, an additional microscopic examination of the resulting wear spots after the tests could be considered.

## REFERENCES

- [1] H. Czichos, *Tribology: A Systems Approach to the Science and Technology of Friction, Lubrication and Wear*, Vol. 1, Elsevier, Amsterdam, 1978.
- [2] P.J. Blau, *Friction Science and Technology: From Concepts to Applications*. New York: CRC Press, 2008.
- [3] B. Bhushan, *Introduction to Tribology*. New York: John Wiley & Sons, 2002.
- [4] F.D. Bowden and D. Tabor, *The Friction and Lubrication of Solids, Part II*. Oxford: Oxford Clarendon Press, 1964.
- [5] I.V. Kragelski, *Friction and Wear*. London: Butterworths, 1965.
- [6] J.F. Archard, *Wear theory and mechanisms*, in: M.B. Peterson, W.O. Winer (Ed.): *Wear Control Handbook*. ASME, New York, pp. 35-80, 1980.
- [7] E. Rabinowicz, *Friction and Wear of Materials*. New York: John Wiley and Sons, 1995.
- [8] K. De Moerlooze, F. Al-Bender and H. Van Brussel, 'An experimental study of ball-on-flat wear on a newly developed rotational tribometer', *Wear*, vol. 271, no. 7-8, pp. 1005-1016, 2011.
- [9] M.A. Chowdhury, M.K. Khalil, D.M. Nuruzzaman and M.L. Rahaman, 'The effect of sliding speed and normal load on friction and wear property of aluminium', *International Journal of Mechanical & Mechatronics Engineering*, vol. 11, no. 1, pp. 45-49, 2011.
- [10] M.A. Chowdhury and D.M. Nuruzzaman, 'Friction coefficient of different material pairs under different normal loads and sliding velocities', *Tribology in Industry*, vol. 34, no. 1, pp. 18-23, 2012.
- [11] M.A. Chowdhury and D.M. Nuruzzaman, 'Experimental investigation on friction and wear properties of different steel materials', *Tribology in Industry*, vol. 35, no. 1, pp. 42-50, 2013.
- [12] J.M. Fildes, S.J. Meyers, C.P. Mulligan and R. Kilaparti, 'Evaluation of the wear and abrasion resistance of hard coatings by ball-on-three-disk test methods – A case study', *Wear*, vol. 302, no. 1-2, pp. 1040-1049, 2013.
- [13] ISO 7148-2, Plain Bearings – Testing of the Tribological Behaviour of Bearing Materials – Part 2: Testing of Polymer-Based Plain Bearing Materials, 2012.
- [14] J.S. Davis, *ASM Specialty Handbook: Copper and Copper Alloys*. Ohio: ASM International, 2001.